FRONTIERS OF PHYSICS

RESEARCH ARTICLE
Volume 19 / Issue 3 / 33203 / 2024

Engineering phonon thermal transport in few-layer $PdSe_2$

Meilin Li, Huanhuan Sun, Jun Zhou, Yunshan Zhao†

Phonon Engineering Research Center of Jiangsu Province, Center for Quantum Transport and Thermal Energy Science, Institute of Physics Frontiers and Interdisciplinary Sciences, School of Physics and Technology, Nanjing Normal University, Nanjing 210023, China
Corresponding author. E-mail: †phyzys@njnu.edu.cn
Received August 7, 2023; accepted September 26, 2023

ABSTRACT

Engineering phonon transport in low-dimensional materials has great significance not only for fundamental research, but also for thermal management applications of electric devices. However, due to the difficulties of micro and nano processing and characterization techniques, the work on tuning phonon transport at nanoscale are scarce. In this work, by introducing Ar^+ plasma, we probed the phonon transport in two-dimensional (2D) layered semiconductor $PdSe_2$ under different defect concentrations. By using thermal bridge method, the thermal conductivity was measured to decrease by 50% after a certain Ar^+ irradiation, which implied a possible phase transition. Moreover, Raman characterizations were performed to show that the Raman sensitive peaks of $PdSe_2$ was red-shifted and finally became disappeared with the increase of defect concentration. "Defect engineering" proves be a practical strategy in tuning the phonon thermal transport in low-dimensional materials, thus providing guidance for potential application in designing thermoelectric devices with various emerging materials.

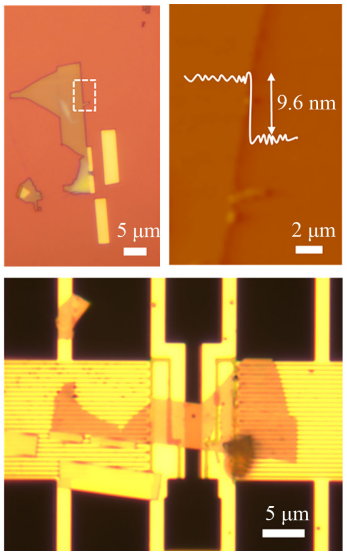

Keywords phonon transport, $PdSe_2$, defects, thermal bridge method

1 Introduction

With the trend of miniaturization and integration of modern electronic devices, how to manage heat effectively becomes a critical issue to improve the performance of electronic devices. Thermoelectric (TE) materials, which can convert heat energy into electricity to reuse waste heat, become an ideal material for thermal management and have been studied extensively [1–3]. The performance of TE materials is determined by the figure of merit (ZT), which is defined as $ZT = S^2\sigma T/\kappa$, where S, σ and κ represents the Seebeck coefficient, electrical conductivity and thermal conductivity, respectively. Obviously, the properties of a high Seebeck coefficient, high electrical conductivity and low thermal conductivity aid to a good ZT value. Due to its tunable bandgaps, special quantum confinement effect, superior electrical conductivity and carrier mobility as well as thickness-dependent thermal conductivity, two-dimensional (2D) materials provide promising candidates to search for excellent TE properties [4–7]. Among the various emerging 2D materials, transitional metal dichalcogenides, TMDCs (MX_2, M = Mo, Pd, W, Ti; X = S, Se) is an important element of van der Waals layered materials [8, 9]. $PdSe_2$ has an unusual quadruple coordination of metal atoms and the two sulfur atoms in the plane are connected by a covalent bond. In a single layer structure, each Pd atom binds to

#Special Topic: Two-dimensional Electronic Materials and Devices (Eds.: Lin Wang & Xiaolong Chen).

Higher Education Press

https://doi.org/10.1007/s11467-023-1351-x

four Se atoms in the same layer and two Pd atoms and three S atoms can form a wrinkled pentagon, which is rather rare in the current materials. As one of the most air-stable TMDCs, $PdSe_2$ shows a high charge carrier mobility and tunable thermal property by external fields, making extensive applications in field-effect transistors, optoelectronic devices [8, 10–13], thermal switches and TE devices [14, 15]. Moreover, the bandgap of $PdSe_2$ can be changed by engineering its thickness and from bulk to monolayer, its bandgap changes from 0 eV to 1.3 eV [13]. Although $PdSe_2$ has shown these interesting physical properties, its phonon thermal transport was studied until recently.

Due to its strong interlayer coupling, the thermal conductivity of $PdSe_2$ shows a thickness-dependent behavior [16–19]. The thermal conductivity of bilayer of $PdSe_2$ grown by CVD is 36.8 $W{\cdot}m^{-1}{\cdot}K^{-1}$ at room temperature measured by Raman characterization, while the thermal conductivity value of few-layer $PdSe_2$ is only 10.1 $W{\cdot}m^{-1}{\cdot}K^{-1}$ [18]. Zhang *et al.* [17] used first-principles calculation to study the acoustic velocity, bandgap and density of states of $PdSe_2$ and demonstrated that the optical modes with low frequencies are increasingly involved in the scattering of acoustic phonons as the number of layers decreases, leading to the decrease of thermal conductivity. Qin *et al.* [19] discovered that monolayer $PdSe_2$ has a low lattice thermal conductivity around 3 $W{\cdot}m^{-1}{\cdot}K^{-1}$ along the x direction at room temperature by the first-principles calculation. Wang *et al.* [20] proposed that $PdSe_2$ can achieve a continuously switchable thermal conductivity through strain-driven structural phase transition. Moreover, due to the low symmetrical pentagonal fold structure, $PdSe_2$ has an anisotropy in lattice structure and thus an anisotropic transport properties [21], and the thermal transport anisotropy ratio as high as 1.42 is demonstrated by micro-Raman thermometry [16].

In semiconductor materials, phonon is the main carriers of heat and its behaviors have a great effect on the thermal conductivity [22–25]. Defects, like vacancies, impurities and dislocations are inevitably introduced in the sample preparation process, and the defect engineering could be further used to modulate the phonon transport. Many studies have used "defect engineering" to regulate the thermal conductivity of 2D materials and investigated the influence of defects on heat transport [26–28]. By controlling the oxygen plasma exposure time, Aiyiti *et al.* [29] tuned the thermal conductivity of MoS_2 to a desired value and observed the transition from crystal to amorphous. Zhao *et al.* [30] studied the change of thermal conductivity of MoS_2 flakes with different defect concentrations under helium ion (He^+) irradiation, and it showed that the Mo vacancy could significantly impede phonon transport compared to that of S vacancy. Wu *et al.* [27] used extensive molecular dynamics simulations to calculate the effects of different types and doses of defects on thermal conductivity of BN and the relationship between phonon-phonon scattering term and phonon-defect scattering term was proposed. For $PdSe_2$, there exist a wide range of binary phases like $Pd_{17}Se_{15}$, Pd_7Se_4 and Pd_4Se, and by laser irradiation, electron beam irradiation, electric field and so on, $PdSe_2$ is expected to undergo phase transition [14, 15]. Among these phases, it has been shown that $Pd_{17}Se_{15}$ is metallic phase and has superconducting behavior, which could be obtained by defect engineering and therefore provides an appropriate approach for engineering phonon transport in $PdSe_2$ [13, 31].

In this work, we study the phonon thermal transport in both intrinsic and defected $PdSe_2$. By wet transfer method, few-layer $PdSe_2$ flake was placed onto a micro-electro-thermal systems (METS) device and the thermal bridge method was employed to measure the thermal conductivity of $PdSe_2$. The Ar^+ was further employed to introduce defects into $PdSe_2$. With increasing the Ar^+ dose, the thermal conductance of $PdSe_2$ kept decreasing until to a critical dose, where the thermal conductance dropped dramatically by 50%. During the Ar^+ irradiation, Raman characterization was carried out as well to record the lattice structure evolution of defected $PdSe_2$, where a possible phase change at the critical dose was observed, corresponding to the change observed in the thermal conductivity. Our work provides a novel approach to tuning the thermal transport in novel 2D materials, enabling further thermal management at nanoscale.

2 Methods

2.1 Preparation of suspended-pad micro-devices

Bulk $PdSe_2$ single crystals were synthesized by a self-flux method as previous reported [32]. Unlike graphene and boron nitride, whose layers are connected by weak van der Waals forces [33, 34], it is challenging to acquire few-layer $PdSe_2$ by mechanical exfoliation due to its strong layer to layer coupling [35]. By using Ar^+ or O^{2+} to bombard clean SiO_2/Si substrates, the interaction force between $PdSe_2$ flakes and substrates was enhanced, and the flake with desired thickness was further obtained. Before transferring onto the pre-patterned suspended thermal bridge device, the atomic force microscope (AFM) is employed to measure the thickness of samples. The thickness of measured $PdSe_2$ sample is 9.6 nm, as shown in Figs. 1(a) and (b).

For the thermal bridge method measurement, there are typically three methods to transfer samples to the devices, including drop-cast method [36], dry/wet transfer method [37] and nano-manipulation method [38]. Considering the operative difficulty and yield, the wet transfer method was used in this study. The substrates with targeted samples were spin-coated with PMMA at

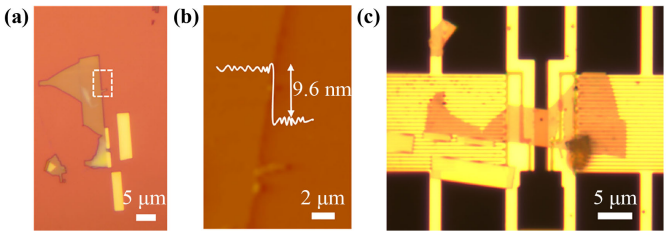

Fig. 1 **(a)** Optical image and **(b)** AFM image of $PdSe_2$. The thickness of the sample is 9.6 nm. **(c)** Optical image of transferred METS sample. Scale bars have been shown in each figure.

the rate of 2000 raps/s with duration of 30 s. Then, the substrates were heated on the hot plates at 100 °C to accelerate the solidification process. The substrates coated with PMMA were then immersed into 20% KOH solution. Under an optical microscope, the marked sample on the suspended PMMA film region was placed on top of the middle of the thermal bridge. Before using acetone to dissolve PMMA, the devices were heated to 120 °C for twenty minutes to well stick the flake with the thermal bridge electrodes. Finally, the critical point dryer (CPD) was used to remove the acetone and the final METS device is shown in Fig. 1(c).

2.2 Thermal bridge measurement

In 2001, the thermal bridge method was firstly used to measure the thermal conductivity of micro- and nano-scale samples [39]. This method can measure not only the thermal conductivity, but also the electric conductivity of nanosheets and nanowires [40–42]. A METS device has two suspended SiN_x membranes with integrated Pt heaters/resistance-thermometers and extra electrodes. One pad is treated as heater and the other sensor. Each pad is connected with six suspended cantilevers to avoid the influence of substrate. During the measurement, a direct current (DC) produced by Keithely 6221 current source meter flows into heater pad to act as a heat source. One part of the heat (Q_1) flows through the suspended cantilevers to the substrate, and the other part (Q_2) flows through the sample to the sensor. Q_1 and Q_2 can be expressed as

$$Q_1 = G_\mathrm{b} \times \Delta T_\mathrm{h}, \tag{1}$$

$$Q_2 = G_\mathrm{s} \times (\Delta T_\mathrm{h} - \Delta T_\mathrm{s}) = G_\mathrm{b} \times \Delta T_\mathrm{s}, \tag{2}$$

where G_b is the thermal conductance of heater membrane. G_s is the thermal conductance of the sample. ΔT_h and ΔT_s is temperature rise of heater and sensor. Under a thermal steady state, G_b and G_s are derived as

$$G_\mathrm{b} = \frac{I^2 \times R_\mathrm{h} + \frac{1}{2} I^2 \times R_\mathrm{L}}{\Delta T_\mathrm{h} + \Delta T_\mathrm{s}}, \tag{3}$$

$$G_\mathrm{s} = \frac{\left(I^2 \times R_\mathrm{h} + \frac{1}{2} I^2 \times R_\mathrm{L}\right) \times \Delta T_\mathrm{s}}{{\Delta T_\mathrm{h}}^2 - {\Delta T_\mathrm{s}}^2}, \tag{4}$$

where R_h and R_L respectively represent the resistance of heater pad and suspended cantilevers. When applying a direct current (DC), the current source meter Keithely 6221 produces a tiny alternating current (AC) at the same time and the lock-in amplifier SR 830 is employed to measure the change of resistance of heater and sensor. Thus, the temperature change is obtained and the thermal conductance of the sample is calculated. During measurement, the thermal bridge device is placed in a high vacuum thermostat with a pressure less than 10^{-5} mbar, which avoids the effect of thermal convection on the measurement. Two Cu covers were employed to reduce the possible thermal radiation inside the thermostat. As shown in Fig. 2(a), the resistance of Pt loops and the temperature coefficient of resistance (TCR) of the measured device can be acquired. Combining Eqs. (3) and (4), G_s and G_b can be obtained, and the thermal conductivity of $PdSe_2$ is further calculated by the following equation:

$$\kappa = G_\mathrm{s} \frac{L}{S} = G_\mathrm{s} \frac{L}{w \times t}, \tag{5}$$

where L, w, and t are the length, width, and thickness of the suspended part of sample, which are 2 μm, 6.5 μm, and 9.6 nm, respectively.

The measurement errors include the temperature drift in the thermostat, the error of sample dimensions, the error in the contact thermal resistance and so on, which can be expressed as

$$\frac{\delta\kappa}{\kappa} = \sqrt{\left(\frac{\delta G}{G}\right)^2 + \left(\frac{\delta L}{L}\right)^2 + \left(\frac{\delta W}{W}\right)^2 + \left(\frac{\delta t}{t}\right)^2 + \left(\frac{\Delta R_c}{R_c}\right)^2}, \tag{6}$$

where R_c is the thermal resistance between samples and thermal bridge devices. Combining the above factors, the uncertainty of the thermal conductivity is obtained accordingly.

3 Results and discussion

By using the thermal bridge method, the temperature dependent thermal conductance was obtained as shown in Fig. 2(b). The thermal conductivity of $PdSe_2$ at room temperature is 9.4±1.1 $\mathrm{W \cdot m^{-1} \cdot K^{-1}}$, consistent with the theoretical calculation [17]. At low temperature, the phonon Umklapp scattering is weak, the mean free path of phonons (MFP) of $PdSe_2$ is mainly limited by defects, boundaries, and so on [43, 44]. Impurities like PMMA residues during the transfer process could contribute as well. As the temperature rises, more and more phonons

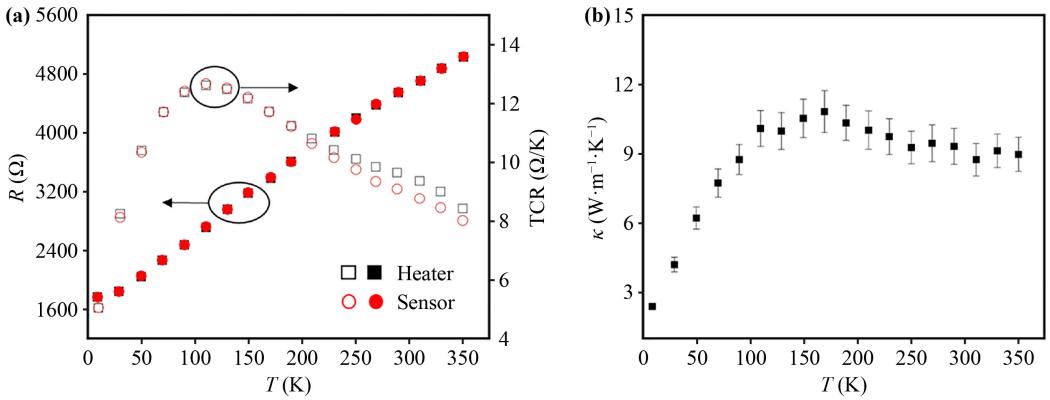

Fig. 2 **(a)** Measured temperature-dependent resistance of heater and sensor and the calculated TCR. **(b)** Intrinsic thermal conductivity of $PdSe_2$. The extracted thermal conductivity ranges from (9.4±1.1) $W{\cdot}m^{-1}{\cdot}K^{-1}$ at room temperature.

are excited and the thermal conductivity of $PdSe_2$ rises. With further increasing the temperature, the thermal conductivity of $PdSe_2$ reaches a maximum value, which is (10.8±0.9) $W{\cdot}m^{-1}{\cdot}K^{-1}$ at a temperature of 170 K as shown in Fig. 2(b). At even high temperature, the phonon Umklapp scattering is enhanced and MFP of phonons is reduced, resulting in decreasing thermal conductivity [37, 45].

In order to tune the thermal conductivity of few-layer $PdSe_2$, the Plasma etching machine was used to introduce defects into $PdSe_2$. Here, we chose Ar^+ with a radio-frequency (RF) power ~ 4 W to well control the concentration of defects. We followed the assumption that per unit time generates the same amount of plasma and the ionized ions uniformly bombard the sample [29]. The measured thermal conductance change with the irradiation time is summarized in Fig. 3, which can be divided into the following parts, as discussed below. Here, we focus on the thermal conductance measured at room temperature.

1) $t < 4$ s: Due to the low Se-Se intralayer bonding energy, $PdSe_2$ is sensitive to defects [13]. As shown in Fig. 3, when the irradiation time was less than 4 s, there was a slight fluctuation in the thermal conductance with increasing the dose. In the meantime, the morphology of the samples did not change under the optical microscope, implying that the thickness of the sample keeps unchanged. The fluctuation of thermal conductance was possibly attributed to both the introduced defects and the removal of impurities. During irradiation, the enhanced phonon-defect scattering resulted in the reduction of thermal conductivity. While some organic impurities may remain on the sample in the transfer process, which can be removed by ionized particle during the bombardment. Thus, it is reasonable that the thermal conductance shows a tiny fluctuation.

2) $t > 4$ s: When the irradiation time was increased to 6 s, the thermal conductance of the sample had a sharp drop around 50%. With further increasing the irradiation

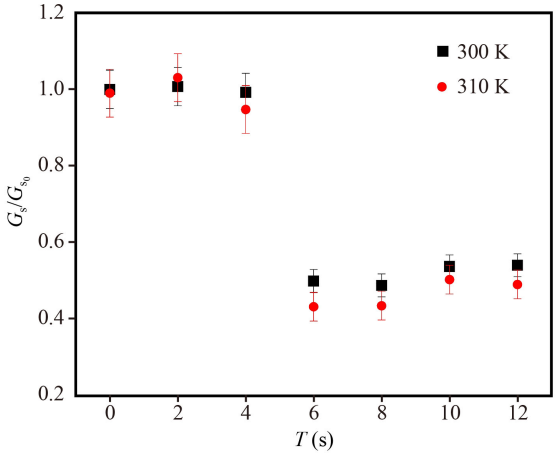

Fig. 3 The thermal conductance of $PdSe_2$ versus the Ar^+ irradiation time at 300 K and 310 K. The thermal conductance of $PdSe_2$ decreases with an increase in the defect concentration.

time, more Se vacancies were created and got concentrated. In this process, the defected $PdSe_2$ would collapse into the other stable phase. According to paper [13], for $PdSe_2$ under Ar^+ irradiation, there exists a phase transition from $PdSe_2$ to $Pd_{17}Se_{15}$. For the metallic phase $Pd_{17}Se_{15}$, the thermal conductance would reach a saturated value as the irradiation time increased further.

In order to further understand the effect of defects on phonon transport, the Raman spectrometer is employed to explore the lattice structure changes of $PdSe_2$ under the introduction of defects. After each thermal measurement under different Ar^+ irradiation, the Raman characterization was performed. The evolutions of Raman spectrum are summarized in Fig. 4. The $PdSe_2$ with a thickness of 9.6 nm showed two sensitive peaks, A_g^1 and A_g^3, which were ~145 and ~255 cm^{-1}, respectively, consistent with the previous experiments [46]. A_g^1 is connected with the in-plane vibration of covalent bond between Pd and Se atoms, and A_g^3 is related to the in-plane vibration of

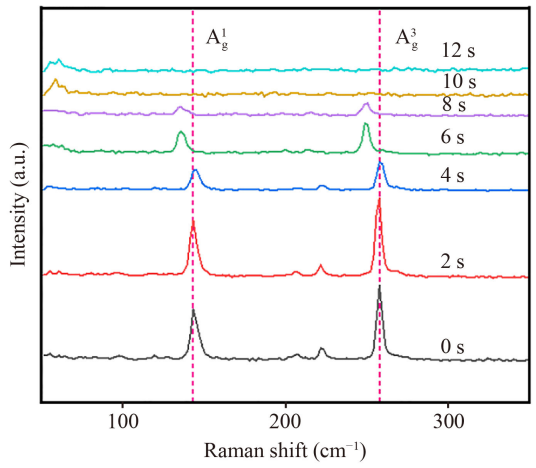

Fig. 4 The evolution of Raman sensitive peaks, A_g^1 and A_g^3, for few layer $PdSe_2$ flakes under various irradiation doses.

two neighboring covalently bonded Se atoms. As the irradiation time increased on a time scale of 0 to 4 seconds, the intensity of these two Raman peaks gradually decreased. The positions of the two modes did not change, indicating that the crystal structure of the sample kept constant. This change coincided with a slight fluctuation in the thermal conductivity. When the time exceeds 4 s, the modes of A_g^1 and A_g^3 showed a slight red-shift and with further increasing the irridiation time, these two peaks almost vanished and at the same time, the thermal conductance reaches a saturated value. The disappearance of Raman peaks suggested the possible phase transition from $PdSe_2$ to $Pd_{17}Se_{15}$. As shown in the work conducted by Akinola *et al.* [13], under the Ar^+ irridiation, semiconductor $PdSe_2$ could change into stable metallic $Pd_{17}Se_{15}$, which could be characterized by low-frequency anti-Stokes peaks (below 50 cm^{-1}). Futher study would be carried out to perform this Raman characterizations for the defected $PdSe_2$.

4 Conclusion

In summary, we experimentally studied the effect of Ar^+ on phonon transport in few-layer $PdSe_2$. By using a wet transfer method, the exfoliated few-layer $PdSe_2$ flakes were transferred onto the pre-patterned suspended thermal bridge devices and the intrinsic thermal conductivity of $PdSe_2$ was measured by the thermal bridge method. By Ar^+ irradiation, defects with different concentrations were introduced into the $PdSe_2$ sample. When the irradiation time is 6s, the thermal conductance of the sample had a sharp drop. Raman spectroscopy was employed to characterize the structure of defected $PdSe_2$, where a phase transition was observed. Our work provides a convenient approach to engineering the thermal transport in 2D layered materials by defects engineering, which can be applied to a broad class of emerging 2D materials for engineering their thermal properties. By introducing defects, the thermal conductivity of $PdSe_2$ is modified, shedding light on the applications of $PdSe_2$ in thermal management, TE energy conversion and so on.

Declarations The authors declare that they have no competing interests and there are no conflicts.

Acknowledgements This work was supported by the National Natural Science Foundation of China (Grant No. 12204244), the Natural Science Foundation of Jiangsu Province (Grant No. BK20210556), and the Department of Science and Technology of Jiangsu Province (No. BK20220032). Y. S. Zhao acknowledges the support from the Jiangsu Specially-Appointed Professor Program.

References

1. Y. Pei, X. Shi, A. LaLonde, H. Wang, L. Chen, and G. J. Snyder, Convergence of electronic bands for high performance bulk thermoelectrics, *Nature* 473(7345), 66 (2011)
2. M. S. Dresselhaus, G. Chen, M. Y. Tang, R. G. Yang, H. Lee, D. Z. Wang, Z. F. Ren, J. P. Fleurial, and P. Gogna, New directions for low-dimensional thermoelectric materials, *Adv. Mater.* 19(8), 1043 (2007)
3. R. Kim, S. Datta, and M. S. Lundstrom, Influence of dimensionality on thermoelectric device performance, *J. Appl. Phys.* 105(3), 034506 (2009)
4. K. Hippalgaonkar, Y. Wang, Y. Ye, D. Y. Qiu, H. Zhu, Y. Wang, J. Moore, S. G. Louie, and X. Zhang, High thermoelectric power factor in two-dimensional crystals of MoS_2, *Phys. Rev. B* 95(11), 115407 (2017)
5. L. D. Hicks and M. S. Dresselhaus, Effect of quantum-well structures on the thermoelectric figure of merit, *Phys. Rev. B* 47(19), 12727 (1993)
6. Y. M. Zuev, W. Chang, and P. Kim, Thermoelectric and magnetothermoelectric transport measurements of graphene, *Phys. Rev. Lett.* 102(9), 096807 (2009)
7. Z. Yu, G. Xiong, and L. Zhang, A brief review of thermal transport in mesoscopic systems from nonequilibrium Green's function approach, *Front. Phys.* 16(4), 43201 (2021)
8. Y. Zhao, P. Yu, G. Zhang, M. Sun, D. Chi, K. Hippalgaonkar, J. T. L. Thong, and J. Wu, Low-symmetry $PdSe_2$ for high performance thermoelectric applications, *Adv. Funct. Mater.* 30(52), 2004896 (2020)
9. Y. Zhao, M. Zheng, J. Wu, X. Guan, A. Suwardi, Y. Li, M. Lal, G. Xie, G. Zhang, L. Zhang, and J. T. L. Thong, Modification of thermal transport in few-layer MoS_2 by atomic-level defect engineering, *Nanoscale* 13(26), 11561 (2021)
10. A. Di Bartolomeo, F. Urban, A. Pelella, A. Grillo, M. Passacantando, X. Liu, and F. Giubileo, Electron irradiation of multilayer $PdSe_2$ field effect transistors, *Nanotechnology* 31(37), 375204 (2020)
11. A. Di Bartolomeo, A. Pelella, X. Liu, F. Miao, M. Passacantando, F. Giubileo, A. Grillo, L. Iemmo, F. Urban, and S. Liang, Pressure-tunable ambipolar conduction and hysteresis in thin palladium diselenide

field effect transistors, *Adv. Funct. Mater.* 29(29), 1902483 (2019)
12. G. D. Nguyen, L. Liang, Q. Zou, M. Fu, A. D. Oyedele, B. G. Sumpter, Z. Liu, Z. Gai, K. Xiao, and A. P. Li, 3D imaging and manipulation of subsurface selenium vacancies in $PdSe_2$, *Phys. Rev. Lett.* 121(8), 086101 (2018)
13. A. D. Oyedele, S. Yang, T. Feng, A. V. Haglund, Y. Gu, A. A. Puretzky, D. Briggs, C. M. Rouleau, M. F. Chisholm, R. R. Unocic, D. Mandrus, H. M. III Meyer, S. T. Pantelides, D. B. Geohegan, and K. Xiao, Defect-mediated phase transformation in anisotropic two-dimensional $PdSe_2$ crystals for seamless electrical contacts, *J. Am. Chem. Soc.* 141(22), 8928 (2019)
14. J. Lin, S. Zuluaga, P. Yu, Z. Liu, S. T. Pantelides, and K. Suenaga, Novel Pd_2Se_3 two-dimensional phase driven by interlayer fusion in layered $PdSe_2$, *Phys. Rev. Lett.* 119(1), 016101 (2017)
15. M. A. ElGhazali, P. G. Naumov, H. Mirhosseini, V. Süß, L. Müchler, W. Schnelle, C. Felser, and S. A. Medvedev, Pressure-induced superconductivity up to 13.1 K in the pyrite phase of palladium diselenide $PdSe_2$, *Phys. Rev. B* 96(6), 060509 (2017)
16. L. Chen, W. Zhang, H. Zhang, J. Chen, C. Tan, S. Yin, G. Li, Y. Zhang, P. Gong, and L. Li, In-plane anisotropic thermal conductivity of low-symmetry $PdSe_2$, *Sustainability (Basel)* 13(8), 4155 (2021)
17. K. C. Zhang, L. Y. Cheng, C. Shen, Y. F. Li, Y. Liu, and Y. Zhu, Thickness-dependent anisotropic transport of phonons and charges in few-layered $PdSe_2$, *Phys. Chem. Chem. Phys.* 23(34), 18869 (2021)
18. T. Jena, M. T. Hossain, and P. K. Giri, Temperature-dependent Raman study and determination of anisotropy ratio and in-plane thermal conductivity of low-temperature CVD-grown $PdSe_2$ using unpolarized laser excitation, *J. Mater. Chem. C* 9(46), 16693 (2021)
19. D. Qin, P. Yan, G. Ding, X. Ge, H. Song, and G. Gao, Monolayer $PdSe_2$: A promising two-dimensional thermoelectric material, *Sci. Rep.* 8(1), 2764 (2018)
20. Y. Wang and J. Ren, Strain-driven switchable thermal conductivity in ferroelastic $PdSe_2$, *ACS Appl. Mater. Interfaces* 13(29), 34724 (2021)
21. A. N. Hoffman, Y. Gu, L. Liang, J. D. Fowlkes, K. Xiao, and P. D. Rack, Exploring the air stability of $PdSe_2$ via electrical transport measurements and defect calculations, *2D Mater. Appl.* 3, 50 (2019)
22. J. Chen, J. He, D. Pan, X. Wang, N. Yang, J. Zhu, S. A. Yang, and G. Zhang, Emerging theory and phenomena in thermal conduction: A selective review, *Sci. China Phys. Mech. Astron.* 65(11), 117002 (2022)
23. Z. Zhang, J. Chen, and B. Li, Negative Gaussian curvature induces significant suppression of thermal conduction in carbon crystals, *Nanoscale* 9(37), 14208 (2017)
24. Y. Cai, M. Faizan, H. Mu, Y. Zhang, H. Zou, H. J. Zhao, Y. Fu, and L. Zhang, Anisotropic phonon thermal transport in two-dimensional layered materials, *Front. Phys.* 18(4), 43303 (2023)
25. C. Yu, Y. Hu, J. He, S. Lu, D. Li, and J. Chen, Strong four-phonon scattering in monolayer and hydrogenated bilayer BAs with horizontal mirror symmetry, *Appl. Phys. Lett.* 120(13), 132201 (2022)
26. K. Bera, A. Roy, D. Chugh, J. Wong-Leung, H. Hoe Tan, and C. Jagadish, Role of defects and grain boundaries in the thermal response of wafer-scale hBN films, *Nanotechnology* 32(7), 075702 (2021)
27. X. Wu and Q. Han, Thermal conductivity of monolayer hexagonal boron nitride: From defective to amorphous, *Comput. Mater. Sci.* 184, 109938 (2020)
28. Q. Cai, D. Scullion, A. Falin, K. Watanabe, T. Taniguchi, Y. Chen, E. J. G. Santos, and L. H. Li, Raman signature and phonon dispersion of atomically thin boron nitride, *Nanoscale* 9(9), 3059 (2017)
29. A. Aiyiti, S. Hu, C. Wang, Q. Xi, Z. Cheng, M. Xia, Y. Ma, J. Wu, J. Guo, Q. Wang, J. Zhou, J. Chen, X. Xu, and B. Li, Thermal conductivity of suspended few-layer MoS_2, *Nanoscale* 10(6), 2727 (2018)
30. Y. Zhao, M. Zheng, J. Wu, X. Guan, A. Suwardi, Y. Li, M. Lal, G. Xie, G. Zhang, L. Zhang, and J. T. L. Thong, Modification of thermal transport in few-layer MoS_2 by atomic-level defect engineering, *Nanoscale* 13(26), 11561 (2021)
31. H. R. Naren, A. Thamizhavel, S. Auluck, R. Prasad, and S. Ramakrishnan, Normal state and superconducting properties of $Rh_{17}S_{15}$ and $Pd_{17}Se_{15}$, *Supercond. Sci. Technol.* 24(10), 105015 (2011)
32. W. L. Chow, P. Yu, F. Liu, J. Hong, X. Wang, Q. Zeng, C. H. Hsu, C. Zhu, J. Zhou, X. Wang, J. Xia, J. Yan, Y. Chen, D. Wu, T. Yu, Z. Shen, H. Lin, C. Jin, B. K. Tay, and Z. Liu, High mobility 2D palladium diselenide field-effect transistors with tunable ambipolar characteristics, *Adv. Mater.* 29(21), 1602969 (2017)
33. J. C. Meyer, A. Chuvilin, G. Algara-Siller, J. Biskupek, and U. Kaiser, Selective sputtering and atomic resolution imaging of atomically thin boron nitride membranes, *Nano Lett.* 9(7), 2683 (2009)
34. D. Pacilé, J. C. Meyer, Ç. Ö. Girit, and A. Zettl, The two-dimensional phase of boron nitride: Few-atomic-layer sheets and suspended membranes, *Appl. Phys. Lett.* 92(13), 133107 (2008)
35. A. D. Oyedele, S. Yang, L. Liang, A. A. Puretzky, K. Wang, J. Zhang, P. Yu, P. R. Pudasaini, A. W. Ghosh, Z. Liu, C. M. Rouleau, B. G. Sumpter, M. F. Chisholm, W. Zhou, P. D. Rack, D. B. Geohegan, and K. Xiao, $PdSe_2$: Pentagonal two-dimensional layers with high air stability for electronics, *J. Am. Chem. Soc.* 139(40), 14090 (2017)
36. J. W. Roh, J. Ham, J. Kim, H. Moon, H. S. Kim, and W. Lee, Extreme reduction of thermal conductivity by embedding Al_2O_3 nanoparticles into single-crystalline Bi nanowires, *Acta Mater.* 136, 315 (2017)
37. C. Wang, J. Guo, L. Dong, A. Aiyiti, X. Xu, and B. Li, Superior thermal conductivity in suspended bilayer hexagonal boron nitride, *Sci. Rep.* 6(1), 25334 (2016)
38. Y. Zhao, M. Zheng, J. Wu, B. Huang, and J. T. L. Thong, Studying thermal transport in suspended monolayer molybdenum disulfide prepared by a nano-manipulator-assisted transfer method, *Nanotechnology* 31(22), 225702 (2020)
39. P. Kim, L. Shi, A. Majumdar, and P. L. McEuen, Thermal transport measurements of individual multiwalled nanotubes, *Phys. Rev. Lett.* 87(21), 215502 (2001)
40. S. Lee, F. Yang, J. Suh, S. Yang, Y. Lee, G. Li, H.

Sung Choe, A. Suslu, Y. Chen, C. Ko, J. Park, K. Liu, J. Li, K. Hippalgaonkar, J. J. Urban, S. Tongay, and J. Wu, Anisotropic in-plane thermal conductivity of black phosphorus nanoribbons at temperatures higher than 100 K, *Nat. Commun.* 6(1), 8573 (2015)

41. I. Jo, M. T. Pettes, E. Ou, W. Wu, and L. Shi, Basal-plane thermal conductivity of few-layer molybdenum disulfide, *Appl. Phys. Lett.* 104(20), 201902 (2014)
42. L. Dong, Q. Xi, D. Chen, J. Guo, T. Nakayama, Y. Li, Z. Liang, J. Zhou, X. Xu, and B. Li, Dimensional crossover of heat conduction in amorphous polyimide nanofibers, *Natl. Sci. Rev.* 5(4), 500 (2018)
43. M. T. Pettes, I. Jo, Z. Yao, and L. Shi, Influence of polymeric residue on the thermal conductivity of suspended bilayer graphene, *Nano Lett.* 11(3), 1195 (2011)
44. J. Lim, K. Hippalgaonkar, S. C. Andrews, A. Majumdar, and P. Yang, Quantifying surface Roughness effects on phonon transport in silicon nanowires, *Nano Lett.* 12(5), 2475 (2012)
45. L. Yang, Y. Tao, Y. Zhu, M. Akter, K. Wang, Z. Pan, Y. Zhao, Q. Zhang, Y. Q. Xu, R. Chen, T. T. Xu, Y. Chen, Z. Mao, and D. Li, Observation of superdiffusive phonon transport in aligned atomic chains, *Nat. Nanotechnol.* 16(7), 764 (2021)
46. W. Luo, A. D. Oyedele, N. Mao, A. Puretzky, K. Xiao, L. Liang, and X. Ling, Excitation-dependent anisotropic Raman response of atomically thin pentagonal $PdSe_2$, *ACS Phys. Chem Au* 2(6), 482 (2022)